Histol Histopathol (2011) 26: 1243-1255

http://www.hh.um.es

Histology and Histopathology

Cellular and Molecular Biology

Pathological correlations between podocyte injuries and renal functions in canine and feline chronic kidney diseases

Osamu Ichii[1], Akira Yabuki[2], Nobuya Sasaki[3], Saori Otsuka[1], Hiroshi Ohta[4], Masahiro Yamasaki[4], Mitsuyoshi Takiguchi[4], Yuka Nami[5], Yoshiharu Hashimoto[5], Daiji Endoh[6] and Yasuhiro Kon[1]

[1]Laboratory of Anatomy, Department of Biomedical Sciences, Graduate School of Veterinary Medicine, Hokkaido University, Sapporo, Japan, [2]Laboratory of Clinical Pathology, Department of Veterinary Sciences, Kagoshima University, Kagoshima, Japan, [3]Laboratory of Laboratory Animal Science and Medicine, Department of Disease Control, Graduate School of Veterinary Medicine, Hokkaido University, Sapporo, Japan, [4]Laboratory of Veterinary Internal Medicine, Department of Veterinary Clinical Sciences, Graduate School of Veterinary Medicine, Hokkaido University, Sapporo, Japan, [5]Office for Faculty Development and Teaching Enriched Veterinary Medicine, Graduate School of Veterinary Medicine, Hokkaido University, Sapporo, Japan and [6]Department of Veterinary Radiology, School of Veterinary Medicine, Rakuno Gakuen University, Hokkaido, Ebetsu, Japan

Summary. Podocytes cover the glomerulus and their adjacent foot processes form a principal barrier called the slit diaphragm. Podocyte dysfunctions, including podocyte loss and slit diaphragm disruptions, induce chronic kidney diseases (CKD). In this study, we analyzed the correlations between podocyte injuries and renal dysfunctions in domestic carnivores. Dogs and cats were divided into normal and CKD groups according to renal histopathology and plasma creatinine values. Immunostaining results showed that linear reactions of slit diaphragm molecules, e.g., nephrin, podocin, and ACTN4, were parallel to glomerular capillaries in all animals. However, in dogs, reactions of nephrin and ACTN4 were changed to a granular pattern in the CKD group, and their intensities significantly decreased with the number of podocytes in the glomerulus. Moreover, the expression of nephrin and ACTN4 negatively correlated with creatinine. Real-time PCR analysis showed that nephrin mRNA expression in the kidneys of CKD dogs was significantly lower than that in normal animals, and negatively correlated with creatinine. Although no significant correlation between renal dysfunction and podocyte injury was detected in cats, histoplanimetric scores of tubulointerstitial lesions in CKD cats were higher than those in both normal cats and diseased dogs. Furthermore, mRNAs of WT1 and SD molecules were detected in urine from CKD animals. In conclusion, podocyte injuries such as podocytopenia and decreased expression of nephrin and ACTN4 in the glomerulus were more strongly correlated with renal dysfunction in dogs than in cats. These findings suggest that the CKD pathogenesis, especially susceptibilities to podocyte injuries, differed between dogs and cats.

Key words: CKD, Podocyte, Dog, Cat

Offprint requests to: Osamu Ichii DVM, PhD, Laboratory of Anatomy, Department of Biomedical Sciences, Graduate School of Veterinary Medicine, Hokkaido University, Kita 18-Nishi 9, Kita-ku, Sapporo 060-0818, Japan. e-mail: ichi-o@vetmed.hokudai.ac.jp

Introduction

In humans, the global population of patients with end-stage renal disease (ESRD) needing dialysis is predicted to reach 21.0 million in the 2010s (Lysaght, 2002). Chronic kidney disease (CKD) progresses to ESRD and can increase the development of risk conditions such as diabetes and hypertension. An increase in the number of CKD patients is seen not only in humans but also in companion animals, as a result of aging. As in humans, CKD is one of most common

Abbreviations: CKD: chronic kidney disease; Cre: creatinine; SD: slit diaphragm; ACTN4: alpha actinin 4; PI3K: phosphoinositide 3-OH kinase; GBM: glomerular basement membrane; PAS: periodic-acid Schiff; TRITC: tetramethylrhodamine isothiocyanate; FITC: fluorescein isothiocyanate; PCR: polymerase chain reaction; TILs: tubulointerstitial lesions; EMT: epithelial-mesenchymal transition

cause of death in dogs and cats. The incidence of CKD is especially high in aged cats (Elliott and Barber, 1998), and the CKD rate has been reported to be 30% in cats over 15 years old (Krawiec and Gelberg, 1989). The prevalence of CKD in dogs has been reported to be 5.8% (Lund et al., 1999). To resolve these serious CKD problems, the National Kidney Foundation and International Renal Interest Society (IRIS) have globally recommended a guideline for the clinicopathological staging of CKD according to urine protein and plasma creatinine (Cre) levels in human and veterinary medicine, respectively (http://www.kidney.org/kidneydisease/ckd/index.cfm; http://www.iris-kidney.com/guidelines/en/index.shtml). Recent studies reported that podocyte injuries in humans are the primary cause of renal pathogenesis (Hara et al., 2010). Podocytes are highly specialized and differentiated cells that cover the glomerular capillary rete through their cytoplasmic processes, called "foot processes". Adjacent foot processes form pores that are covered by a zipper- and membrane-like structure called the slit diaphragm (SD). Recent studies have identified several component molecules of SD, such as nephrin, podocin, and alpha actinin 4 (ACTN4). Several studies reported that loss of podocytes (podocytopenia) is correlated with the development of glomerulopathy (Suzuki et al., 2009) and their deciduation to urine is confirmed by the presence of urinary SD molecules (Sato et al., 2009; Hara et al., 2010).

Nephrin is a major transmembrane protein of SD and is coded by the gene nephrosis 1, congenital, Finnish type (*NPHS1*; chromosome 19 [human] or 1 [dog]). *NPHS1* mutation was found in congenital nephrotic syndrome of the Finnish type (Patrakka et al., 2000). Furthermore, nephrin-deficient models showed foot process enfacement with proteinuria (Juhila et al., 2010). Interestingly, nephrin also participates in cell signaling and interacts with the p85 regulatory subunit of phosphoinositide 3-OH kinase (PI3K), recruits PI3K to the plasma membrane and stimulates PI3K-dependent AKT signaling, controlling cell growth, migration, and survival (Huber et al., 2003). Podocin is a member of the somatin protein family and localizes to the podocyte foot process membrane at the insertion site of SD. It is coded by the gene nephrosis 2, idiopathic, steroid-resistant (*NPHS2*; chromosome 1 [human] or 7 [dog]). In humans, *NPHS2* mutation is associated with autosomal recessive steroid-resistant nephritic syndrome (Caridi et al., 2005). Nphs2$^{-/-}$ mice develop proteinuria with massive mesangial sclerosis (Roselli et al., 2004). ACTN4 (coded by *ACTN4*; chromosome 19 [human] or 1 [dog]) is an actin-bundling protein and plays an important role in stabilizing the podocyte cytoskeleton structure by connecting actin filaments. *ACTN4* mutations are associated with the development of familial focal segmental glomerulosclerosis (Kaplan et al., 2000). *In vitro*, ACTN4-deficient podocytes were less adherent than wild-type cells to the glomerular basement membrane (GBM) components, collagen IV and laminins 10 and 11 (Dandapani et al., 2007).

Quantitative changes of SD molecules also cause glomerular diseases in experimental animal models. Puromycin aminonucleoside-induced nephropathy in a rat model of minimal change nephrotic syndrome showed a decrease in nephrin mRNA and change in protein localizations from a linear to a granular pattern in the glomerular capillary (Luimula et al., 2000). Therefore, altered expression of SD molecules has a large impact on the pathogenesis of glomerular injuries in humans and laboratory animals. However, no experimental evidence exists on companion animals due to the scarcity of both renal biopsy and necropsy samples in veterinary medicine. In the present study, podocyte injuries were analyzed, with focus on podocytopenia and expression changes of SD molecules in CKD of dogs and cats. Finally, we considered podocyte injuries more closely related to CKD in dogs than in cats, and emphasized the importance of pathogenic species-specific differences in veterinary nephrology.

Materials and methods

Animals and tissue preparations

Kidney samples from dogs (n=34, approximately 2-20 years) and cats (n=21, approximately 6 months–17 years) were obtained from postmortem examinations or other surgical and internal experiments in Kagoshima University and Hokkaido University, Japan. Experiments in this study were performed in accordance with the *Guidelines for Animal Experimentation of Kagoshima University and the Guide for the Care and Use of Animals of the School of Veterinary Medicine, Hokkaido University* (the latter is approved by the Association for Assessment and Accreditation of Laboratory Animal Care International). Plasma Cre values were obtained from clinical analysis. Collected kidney samples were fixed in formaldehyde-based reagents. After a thorough washing in 0.1 M phosphate buffer (pH 7.4), samples were embedded in paraffin according to the standard procedure. The samples were cut into 2-μm-thick sections and subsequently treated with periodic acid Schiff (PAS). Parts of the sections were analyzed by immunohistochemistry or immunofluorescence studies. The remaining paraffin blocks were stored for analysis of mRNA expression.

The development of CKD in dogs and cats were judged from the diagnosis of a clinical veterinarian, renal histopathological findings of kidneys sections, and values of plasma Cre. According to the IRIS staging system on the basis of plasma Cre levels (http://www.iris-kidney.com/guidelines/en/index.shtml), CKD stages of animals are divided into stage 1 (<1.4 mg/dL in dogs, <1.6 mg/dL in cats), stage 2 (1.4-2.0 mg/dL in dogs, 1.6-2.8 mg/dL in cats), stage 3 (2.1-5.0 mg/dL in dogs, 2.9-5.0 mg/dL in cats), and stage 4 (>5.0 mg/dL in dogs and cats). Animals showing no renal injury and

dysfunction were defined as normal, and all dogs and cats were divided into the normal and CKD groups.

Immunostaining methods

The immunohistochemical procedure involved the following steps: deparaffinization and rehydration; antigen retrieval by heating the sample in a 10 mM citrate buffer (pH 6.0) in an autoclave at 105°C for 15 min; treatment with 3% H_2O_2 in methanol for 15 min; washing in 10 mM phosphate-buffered saline (PBS; pH 7.4); blocking with 0.25% casein in PBS for 60 min; overnight incubation at 4°C with rabbit anti-human WT1 antibodies (Santa Cruz) at a 1:800 dilution, rabbit anti-human podocin antibodies (SIGMA) at a 1:200 dilution, goat anti-human nephrin antibodies (Santa Cruz) at a 1:100 dilution, and rabbit anti-human ACTN4 antibodies (SIGMA) at a 1:400 dilution; washing in PBS; incubation for 30 min at room temperature with nondiluted biotinylated anti-rabbit IgG (Nichirei) or donkey biotinylated anti-goat IgG (Santa Cruz) diluted at 1:100; washing in PBS; incubation for 30 min with peroxidase-conjugated streptavidin (Nichirei); washing in PBS; detection of immunoreactivity using 3,3'-diaminobenzidine (DAB) (Wako); and termination of the reaction with distilled water. The sections were counterstained using Carazzis' hematoxylin.

For double-staining analysis, an immunofluorescence experiment was performed after antigen retrieval with citrate buffer and casein blocking. In the first reaction, goat anti-human nephrin antibodies and tetramethylrhodamine isothiocyanate (TRITC)-conjugated rabbit anti-goat IgG antibodies (Zymed), both at 1:100 dilution, were used. For double staining with podocin and ACTN4, rabbit anti-podocin antibodies at 1:200 dilution, rabbit anti-ACTN4 antibodies at 1:400 dilution, and fluorescein isothiocyanate (FITC)-conjugated goat anti-rabbit IgG antibodies (Zymed) at 1:100 dilution were used. The sections were examined under a fluorescence microscope (FSX100; Olympus).

Histoplanimetric analysis

In histological sections, renal corpuscles with the vascular or urinary pole were selected and investigated at renal cortices bordered by arcuate arteries and veins from the renal medulla. First, based on the Weibel and Gomez method (White and Bilous, 2004), the number of WT1-positive cells in the glomerulus (over 6 glomerulus) was counted, and these values were divided by the area of the glomerulus. Finally, the mean value in each animal was expressed as an index of the podocyte number. For quantifications of positive immunohistochemical reactions of SD molecules, binary digital figures of the sections were prepared. Briefly, positive reactions of SD molecules in the glomerulus and other cell components were changed to black and white, respectively, by means of GNU Image Manipulation Program 2.2.6 (GIMP, free software: http://www.gimp.org/). In 1 renal corpuscle, the areas of glomerulus and black pixels of positive reaction were measured by means of Image J 1.43 (free software: http://rsbweb.nih.gov/ij/index.html). Finally, the number of pixels per area was calculated for each SD molecule.

To assess the severity of tubulointerstitial lesions (TILs), 10 areas per kidney were examined using PAS-stained sections and scored according to the following criteria: grade 0, no recognizable lesion was observed; grade 1, a few mononuclear cells infiltrated into the tubulointerstitium; grade 2, mild cell infiltrations were observed in the tubulointerstitium; grade 3, dilations or atrophy of renal tubules were observed in addition to grade 2 lesions; grade 4, severe cell infiltrations were observed in addition to tubular dilations or atrophy; grade 5, tubulointerstitial fibrosis was observed. Finally, the mean grade in each animal was expressed as the TIL score.

Electron microscopy

For transmission electron microscopy, a part of the kidney samples was fixed in a mixture of 2.5% glutaraldehyde and 2% paraformaldehyde, postfixed in osmium tetroxide, dehydrated in a graded alcohol series, and finally embedded in Quetol 812 (Nisshin EM). Ultrathin sections (40 nm) were double stained with uranyl acetate and lead citrate.

Reverse transcription and real-time polymerase chain reaction

To obtain total RNAs, 50-μm-thick sections from stocked paraffin blocks were prepared and collected into 1.5-mL tubes. These sections were deparaffinized by fresh xylene. After 1-min incubation, half volume of 99.5% ethanol was added to the tubes and the solution was mixed well. Samples were centrifuged at 15 000 rpm for 2 min. The mixture of xylene and ethanol was discarded, and fresh 99.5% ethanol was added. After centrifugation, ethanol was discarded and precipitated materials were dried. Precipitated samples were treated with 0.1 mg/mL Proteinase K (Wako) solution (10 mM Tris-HCl [pH 7.4], 5 mM EDTA, 1% SDS) for 15 min at 50°C. TRIzol reagent (Invitrogen) was added to the samples, and the solution was mixed. After 5 min, chloroform was added to the samples and mixed. After 3 min, the mixed solutions were centrifuged at 15 000 rpm for 15 min at 4°C. Supernatant fluid was transferred to other tubes, and standard isopropanol precipitation was performed. To detect the urine mRNA, total RNAs were purified by using RNAqueous Kit (Ambion) from urine sediments obtained from the centrifuged 300-μL urine. Purified total RNAs were treated with DNase for DNA digestion (Nippon Gene) and synthesized to cDNAs by using ReverTra Ace (Toyobo) and Random Primer (Promega).

Quantitative real-time polymerase chain reaction

(PCR) analysis was performed using Brilliant SYBR Green QPCR Master Mix (Stratagene) and a real-time thermal cycler (MX 3000; Stratagene). The primer sequences were from UCSC Genome Bioinformatics (http://genome.ucsc.edu/), Entrez cross-database search (http://www.ncbi.nlm.nih.gov/sites/gquery), or Ensembl Genome Browser (http://uswest.ensembl.org/index.html). Details of primer applications are summarized in Table 2. In cats, primers for undetermined genes were constructed based on highly homologous regions in dogs, as determined by homology analyses of human, cow, dog, and mouse genomes. The amplification conditions were as follows: 10 min at 95°C; 40 cycles of 10 s at 95°C, 20 s at 58°C, and 20 s at 72°C; 1 cycle of 10 s at 95°C, 20 s at 58°C, and 20 s at 95°C. ROX dye was included in each reaction to normalize non-PCR-related fluctuations in fluorescence signals. The amplification specificity of all PCR reactions was confirmed by melting curve analysis. Nontemplate controls were included for each primer pair to assess any significant level of contaminants. Quantitative data of target genes were normalized to ACTB expression.

Statistical analysis

Results were expressed as mean (standard error) and statistically analyzed using nonparametric Mann-Whitney *U* test ($P<0.05$). Correlation between 2 parameters was analyzed using Spearman's correlation test ($P<0.05$).

Results

Renal histopathology

All animals were divided into normal and CKD groups according to Cre values and renal histopathology with PAS-stained sections (Table 1, Fig. 1). Histopathological changes in kidneys differed between dogs and cats. In diseased dogs and cats, glomerular hypertrophy, expansion of the mesangial matrix, and thickening of the GBM were commonly observed (Fig. 1). In some cases, proliferation of mesangial and endothelial cells, spike-like alternations, or a double contours of the GBM were observed (data not shown). In cases with severe renal dysfunctions, TILs, such as infiltration of mononuclear cells and fibrosis, were observed in both animals; however, these lesions were more common in cats than in dogs (Fig. 1e and f). Briefly, CKD cats showed TILs in earlier CKD stages compared to dogs (Fig. 1b,e). In the histoplanimetry of TILs, CKD cats showed significantly higher values than normal cats and CKD dogs, and significant differences were also observed between normal and CKD dogs (Fig. 1g).

Glomerular localizations of WT1 and SD molecules

Adjacent foot processes forming the pores that are covered by the linear SD structure were observed by electron microscopy (Fig. 2a). Fig. 2b also shows the schema of the localization of SD-associated molecules. In podocytes of CKD dogs, foot process effacements were clearly observed, and their GBM was thickened and waved (Fig. 2c,d). The podocytes of these animals tend to drop to the capsular lumen, and adhesions between podocytes and the GBM were loose (Fig. 2e,f).

By immunohistochemistry, WT1-positive nuclei (markers for podocytes) were observed in the glomerulus of both normal and CKD animals; however, these nuclei were found in greater numbers in normal animals (Fig. 3a,i) than in CKD animals (Fig. 3e,m). Linear positive reactions of nephrin, podocin, and ACTN4 were observed parallel to the glomerular capillary rete in both normal and CKD animals (Fig. 3b-d,f-h,j-l,n-p). In particular, positive reactions of nephrin and ACTN4 in diseased animals were weaker than those in normal animals, especially in dogs (Fig. 3f,h). On the other hand, podocin changes in relation to CKD were immunohistochemically unclear in both dogs and cats (Fig. 3c,g,k,o).

To elucidate the details of glomerular SD localizations in dogs, immunofluorescence studies were performed (Fig. 4). Clear linear reactions of nephrin, podocin, and ACTN4 were observed parallel to the glomerular capillary rete in the normal groups (Fig. 4a-c,g-i). However, the reaction of SD molecules in CKD dogs was changed from a linear pattern to irregular and granular ones, and their reaction intensities, especially nephrin and ACTN4, were weaker in CKD animals than in the normal groups (Fig. 4d-f,j-l).

Quantitative correlations between podocyte injuries

The expression of proteins was histoplanimetrically analyzed by using immunohistochemical sections (Fig. 5). First, to evaluate podocytopenia in CKD, the number of WT1-positive cells per glomerular area (index for podocyte numbers) were counted in renal cortices (Fig. 5a). CKD dogs and cats had smaller numbers of WT1-positive cells per glomerular area than the normal animals. Statistically significant differences were observed in dogs (Fig. 5a). A significant decrease of nephrin expression in glomeruli was observed histoplanimetrically in dogs (Fig. 5b). On the other hand, no difference of podocin expression was observed among animal species and groups (Fig. 5c). The histoplanimetry of ACTN4 expression in glomeruli showed that a significant decrease was observed in dogs (Fig. 5d). In CKD cats, although the number of WT1-positive cells per glomerular area, and the histoplanimetric scores of nephrin and podocin tended to decrease compared to normal cats, no significant differences were detected in this study.

To analyze mRNA expression, real-time PCR analysis was performed (Fig. 6). In the dog CKD group, the expression of *WT1*, *NPHS1* (nephrin), and *NPHS2* (podocin) tended to decrease compared to that in the normal group (Fig. 6a,b,d). Significant differences were

Table 1. The clinical informations of animals.

Name	Sex	Strain	Age (year)	Cre (mg/dl)	CKD	Application
Dog						
C1	M	Mix	13.0	3.3	Stage3	Histo, mRNA
C2	Sp	Golden Retriever	7.5	3.8	Stage3	Histo, mRNA
C3	M	Shiba	20.0	3.1	Stage3	Histo, mRNA
C4	M	Mix	15.0	4.8	Stage3	Histo, mRNA
C5	F	Tosa	N	0.3	Normal	Histo, mRNA
C6	F	Mix	18.0	0.4	Stage1	Histo, mRNA
C7	Ca	Mix	N	0.6	Normal	Histo, mRNA
C8	Sp	Mix	15.0	10.5	Stage4	Histo, mRNA
C9	N	Beagle	N	0.6	Normal	Histo, mRNA
C10	F	Labrador Retriever	8.0	1.0	Normal	Histo, mRNA
C11	M	Chihuahua	4.0	2.6	Stage3	Histo, mRNA
C12	M	Labrador Retriever	6.0	1.5	Stage2	Histo, mRNA
C13	N	Beagle	N	0.6	Normal	Histo, mRNA
C14	N	Beagle	N	0.7	Normal	Histo, mRNA
C15	N	Akita	N	0.7	Normal	Histo, mRNA
C16	N	Mix	N	6.6	Stage4	Histo, mRNA
C17	Ca	Mix	6.0	0.2	Normal	Histo, mRNA
C18	M	Beagle	N	0.7	Normal	Histo, mRNA
C19	M	Beagle	N	0.5	Normal	Histo, mRNA
C20	M	Beagle	N	0.7	Normal	Histo, mRNA
C21	M	Beagle	N	0.5	Normal	Histo, mRNA
C22	M	Beagle	N	0.4	Normal	Histo, mRNA
C24	F	Mix	14.4	5.3	Stage4	Urine
C25	M	Yorkshire Terrier	13.0	1.8	Stage2	Urine
C26	F	Welsh Corgi	13.0	1.8	Stage2	Urine
C27	M	Mix	12.0	1.2	Stage1	Urine
C28	M	Dachshund	12.0	1.5	Stage2	Urine
C29	F	Mix	12.0	0.8	Stage1	Urine
C30	F	Border Collie	1.0	1.5	Stage2	Urine
C31	M	Shetland Sheepdog	10.0	2.5	Stage3	Urine
C32	N	West Highland White Terrier	N	2.3	Stage3	Urine
C33	M	Border Collie	9.0	1.4	Stage2	Urine
C34	F	Mix	21.0	3.1	Stage3	Urine
Cat						
F1	M	Mix	N	1.6	Stage2	Histo, mRNA
F2	Ca	Mix	10.0	8.7	Stage4	Histo, mRNA
F3	F	Mix	<1.0	0.7	Normal	Histo, mRNA
F4	Sp	Mix	17.0	1.2	Normal	Histo, mRNA
F5	Ca	Mix	8.0	0.8	Normal	Histo, mRNA
F6	M	Mix	N	2.0	Stage2	Histo, mRNA
F7	F	Mix	15.0	2.9	Stage3	Histo, mRNA
F8	N	N	N	12.4	Stage4	Histo, mRNA
F9	Ca	Mix	13.0	1.4	Normal	Histo, mRNA
F10	F	Mix	N	1.2	Normal	Histo, mRNA
F11	N	Abyssinian	7.0	1.3	Stage1	Urine
F12	N	Persian	3.0	1.8	Stage2	Urine
F13	N	Mix	14.0	0.7	Stage1	Urine
F14	N	Mix	16.0	3.7	Stage3	Urine
F15	N	Scottish Fold	5.0	1.9	Stage2	Urine
F16	N	Mix	N	9.9	Stage4	Urine
F17	N	Russian Blue	N	0.5	Stage1	Urine
F18	N	Mix	N	3.0	Stage3	Urine
F19	N	Mix	15.0	2.4	Stage2	Urine
F20	N	Mix	N	20.0	Stage4	Urine
F21	N	Abyssinian	6.0	2.9	Stage3	Urine

BW: Body Weights, BUN: Blood Urea Nitrogen, Cre: Creatinine, M: Male, F: Female, Ca: Castrated, Sp: Spay, N: Unknown, CKD: Chronic Kidney Disease, Histo: Histopathological analysis, mRNA: real-time PCR analysis. Urine: Urinary mRNA analysis.

Table 2. Details of gene specific primers.

Gene name	Symbol	Reference	Sequence	Predicted size	Application
Wilms tumor 1	*WT1*	ENSCAFT00000011914	F: CAGGTGTGAAACCATTCCAG R: CCAGCTGGAGTTTGGTCATG	210bp	Real-time PCR for dog
nephrosis 1, congenital, Finnish type	*NPHS1*	XM_541685	F: CCTGTATGATGAAGTGGAAAGG R: AGGGTCCAAGTTTCCTGCTAC	157bp	Real-time PCR for dog
		Hu, Bo, Ca, Mu	F: TGGAAGCCTGGCTTTGATG R: CCTGTATCGTGTAGAAGGCT	150bp	Real-time PCR for cat
nephrosis 2, idiopathic, steroid-resistant	*NPHS2*	XM_547443	F: GCCCAAGATCTAAAGGTTGC R: ACAGCCAGTGAGTGCTGAAG	116bp	Real-time PCR for dog
		Hu, Bo, Ca, Mu	F: CTGTGAGTGGCTTCTTGTCCTC R: GGAAGCAGATGTCCCAGTCG	132bp	Real-time PCR for cat
actinin, alpha 4	*ACTN4*	XM_862305	F: ACTACATGGCCCAGGAAGAC R: AAATGACCTCCAGGAGAAGC	186bp	Real-time PCR for dog
actin, beta	*ACTB*	ENSCAFT00000025413	F: ACCTCTATGCCAACACAGTGC R: ACACAGAGTACTTGCGCTCAG	144bp	Real-time PCR for dog

F: forward; R: reverse; Hu, Bo, Ca, Mu: primers were dezined based on canine (Ca) sequences at high homology resions among human (Hu), bovine (Bo), Ca, and murine (Mu).

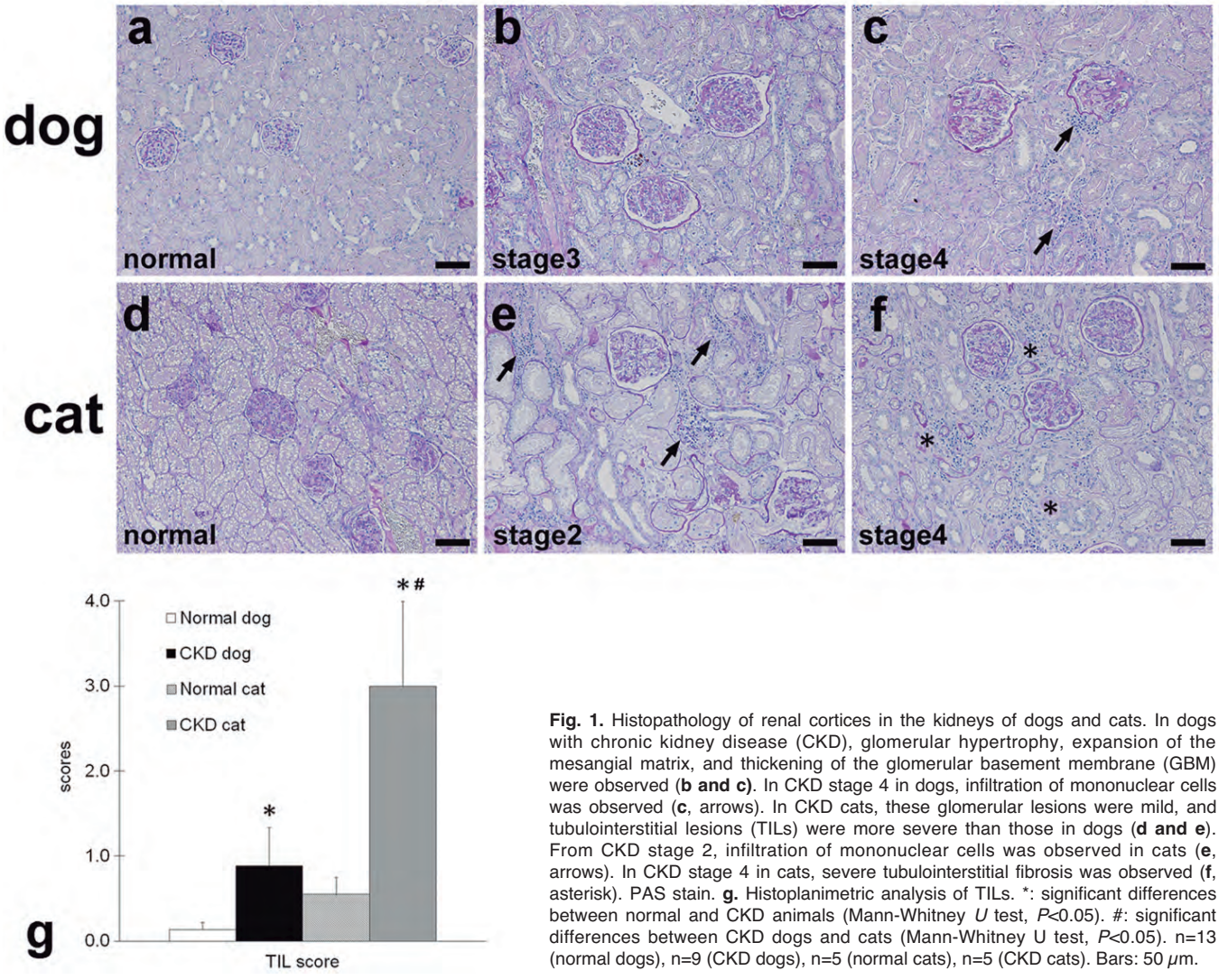

Fig. 1. Histopathology of renal cortices in the kidneys of dogs and cats. In dogs with chronic kidney disease (CKD), glomerular hypertrophy, expansion of the mesangial matrix, and thickening of the glomerular basement membrane (GBM) were observed (**b and c)**. In CKD stage 4 in dogs, infiltration of mononuclear cells was observed (**c**, arrows). In CKD cats, these glomerular lesions were mild, and tubulointerstitial lesions (TILs) were more severe than those in dogs (**d and e**). From CKD stage 2, infiltration of mononuclear cells was observed in cats (**e**, arrows). In CKD stage 4 in cats, severe tubulointerstitial fibrosis was observed (**f**, asterisk). PAS stain. **g.** Histoplanimetric analysis of TILs. *: significant differences between normal and CKD animals (Mann-Whitney *U* test, $P<0.05$). #: significant differences between CKD dogs and cats (Mann-Whitney U test, $P<0.05$). n=13 (normal dogs), n=9 (CKD dogs), n=5 (normal cats), n=5 (CKD cats). Bars: 50 μm.

Table 3. Correlations between the protein and mRNA expressons of podocyte injury markers and renal function.

Dogs	WT1	nephrin	podocin	ACTN4
Cre vs protein	r=-0.411, *P*=0.064	r=-0.434*, *P*=0.049*	r=-0.173, *P*=0.453	r=-0.496*, *P*=0.022*
Cre vs mRNA	r=-0.277, *P*=0.212	r=-0.473*, *P*=0.026*	r=-0.124, *P*=0.582	r=-0.310, *P*=0.890
Cats	**WT1**	**nephrin**	**podocin**	**ACTN4**
Cre vs protein	r=-0.492, *P*=0.148	r=-0.393, *P*=0.261	r=-0.084, *P*=0.818	r=0.503, *P*=0.138
Cre vs mRNA	r=-0.583, *P*=0.099	r=-0.310, *P*=0.417	r=-0.276, *P*=0.472	r=-0.417, *P*=0.265

Cre: plasma creatinine, WT1: Wilms tumor 1, ACTN4: actinin, alpha 4, *: Spearman's correlation test (*P*<0.05), n=22 (dogs), n=10 (cats). Values of protein expressions are based on histoplanimetric scores.

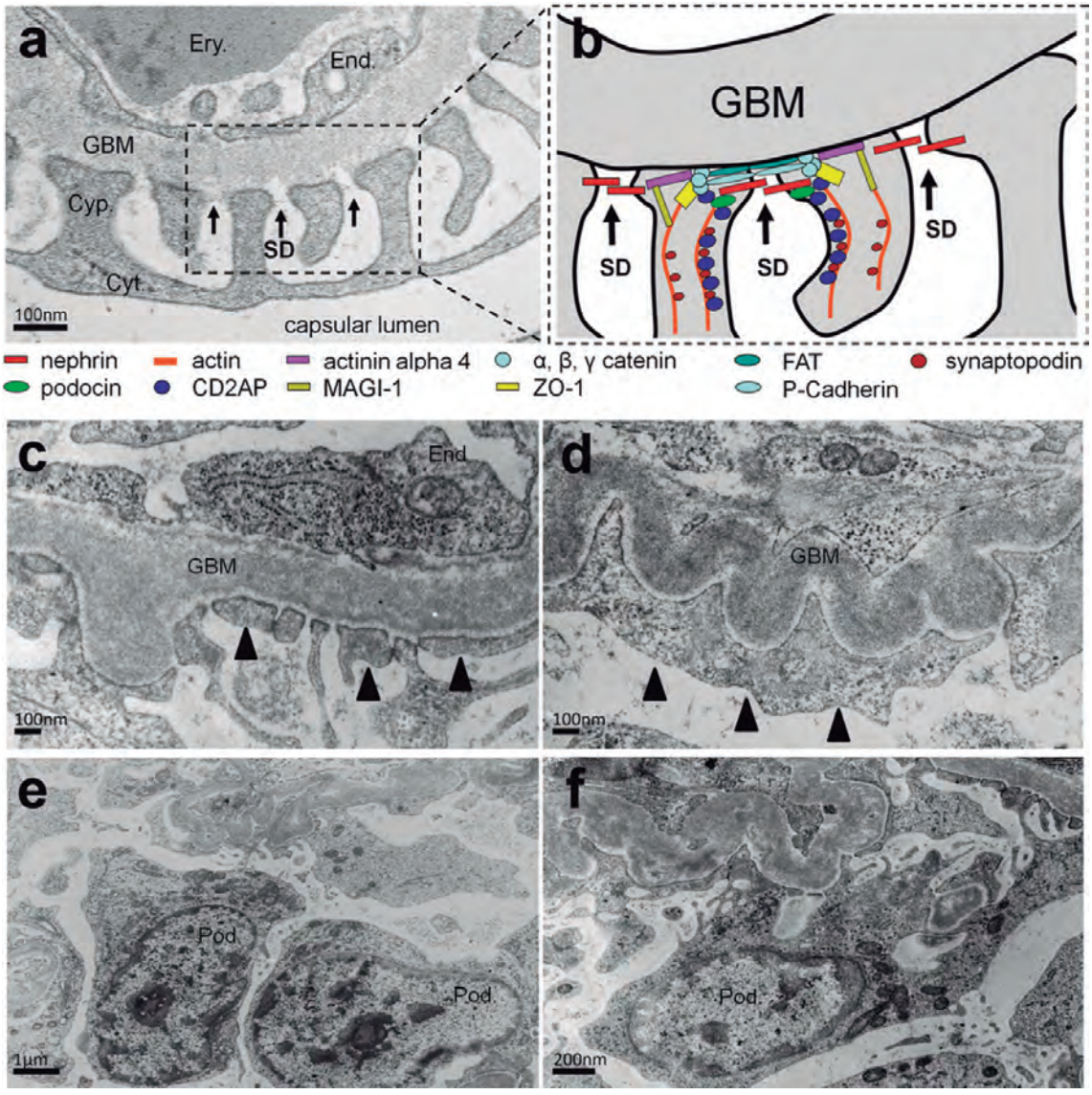

Fig. 2. Structures of the slit diaphragm (SD) in the glomerulus. Normal glomerulus of dog **(a)**. Schema of SD and its associated molecules **(b)**. The podocytes cover the glomerular capillary rete through their cytoplasmic processes called "foot processes (=cytopodium of podocyte: Cyp)". Adjacent foot processes form the pores that are covered by a zipper- and membrane-like structure, SD (**a and b**, arrows). **c-f.** Electron micrographs of the glomerulus in CKD dogs. Foot process effacements are observed (**c and d**, arrowheads), and the GBM is thickened and waved (**c and d**). Podocytes of CKD dogs tend to drop to the capsular lumen, and cell adhesions between podocytes and the GBM are loose (**e and f**). Ery.: erythrocyte, End.: endothelial cell, Cyt.: cytotrabecula of podocyte, Cyp.: cytopodium of podocyte, Pod.: podocyte.

Table 4. Correlations between the idices of podocyte number and protein and mRNA expressions of podocyte markers.

Dogs	nephrin	podocin	ACTN4
Podocyte index vs protein	r=0.532*, *P*=0.016*	r=0.414, *P*=0.069	r=0.334, *P*=0.150
Podocyte index vs mRNA	r=0.454*, *P*=0.339*	r=-0.339, *P*=0.143	r=-0.407, *P*=0.084
Cats	**nephrin**	**podocin**	**ACTN4**
Podocyte index vs protein	r=0.654*, *P*=0.040*	r=0.123, *P*=0.734	r=0.464, *P*=0.177
Podocyte index vs mRNA	r=0.026, *P*=0.947	r=-0.315, *P*=0.409	r=0.167, *P*=0.668

Podocyte index: WT1-positive cells/glomerular area: WT1: Wilms tumor 1, ACTN4: actinin, alpha 4, *: Spearman's correlation test (*P*<0.05), n=22 (dogs), n=10 (cats). Values of protein expressions are based on histoplanimetric scores.

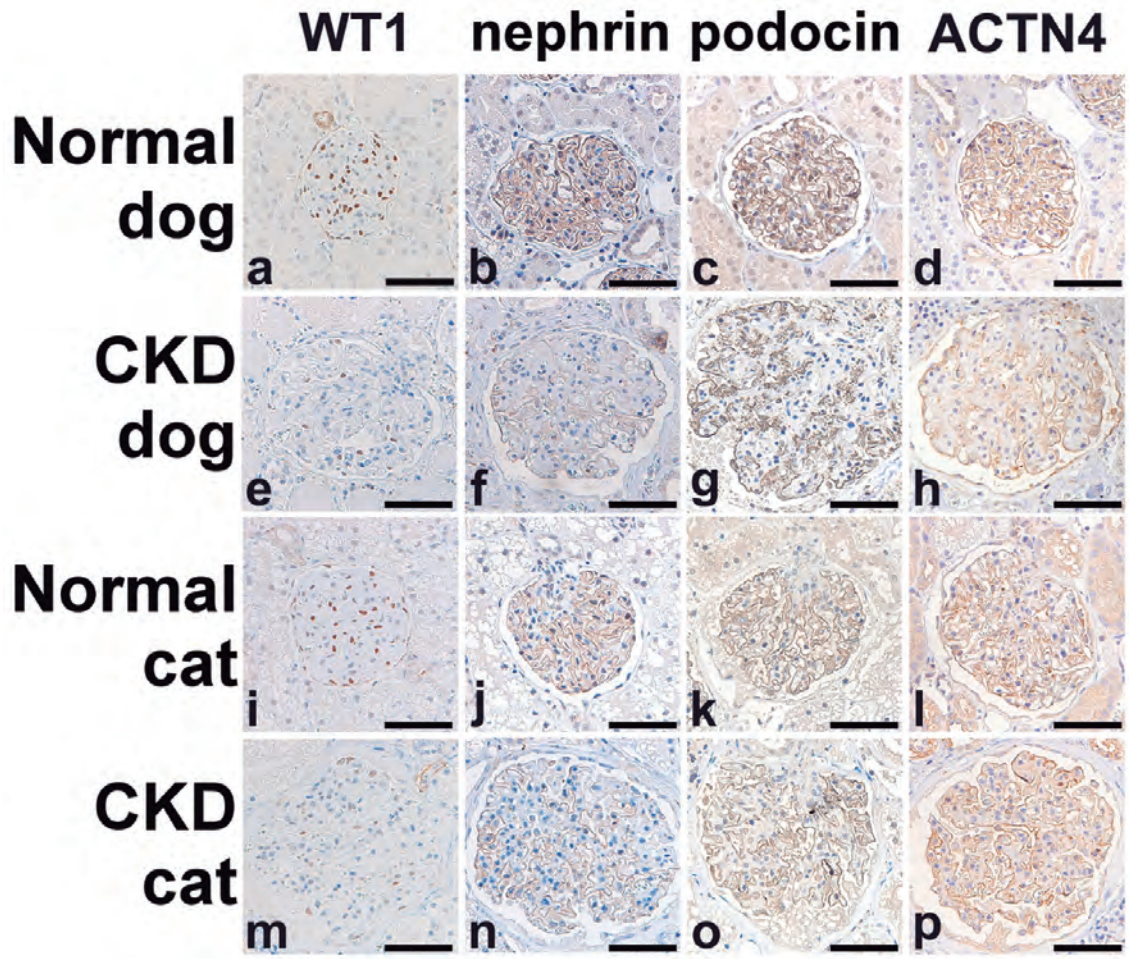

Fig. 3. Localizations of WT1 and SD molecules in the kidneys of dogs and cats. **a-p.** Light micrographs of renal corpuscles in immunohistochemical staining sections of dogs and cats. WT1-positive reactions localized to the nucleus of glomerular podocytes in both normal and CKD animals (**a, e, i, and m**). The number of WT1-positive nuclei in CKD animals tended to decrease compared to those in normal animals, especially in dogs (**a and e)**. Linear positive reactions of nephrin, podocin, and ACTN4 were observed parallel to the glomerular capillary in both normal and CKD animals (**b-d, f-h, j-l, and n-p)**. The positive reactions of nephrin and ACTN4 in CKD animals were weaker than in those in normal animals, especially in dogs (**f and h**). For immunoreactions of podocin, no remarkable change was observed between normal and CKD animals (**c, g, k, and o)**. Bars: 50 μm.

especially observed in *NPHS1* expression (Fig. 6b). On the other hand, in cats, although the expression of *WT1* and *NPHS2* tended to decrease in the CKD group, no significant difference was detected (Fig. 6e-h).

Pathological correlations between podocyte injuries and renal functions

Table 3 summarizes the results of correlation analysis between the indices of podocyte injuries and renal functions. In dogs, Cre was negatively correlated with histoplanimetric scores of nephrin (r -0.434, P=0.049) and ACTN4 (r=-0.496, P=0.022). In dog kidneys, Cre was also negatively correlated with *NPHS1* mRNA expression (r=-0.473, P=0.026). In cats, although negative correlations between Cre and histoplanimetric scores of WT1, nephrin, and podocin were observed, these correlations were weaker than those in dogs, and no significant difference was observed. Similar results were obtained from correlations between Cre and

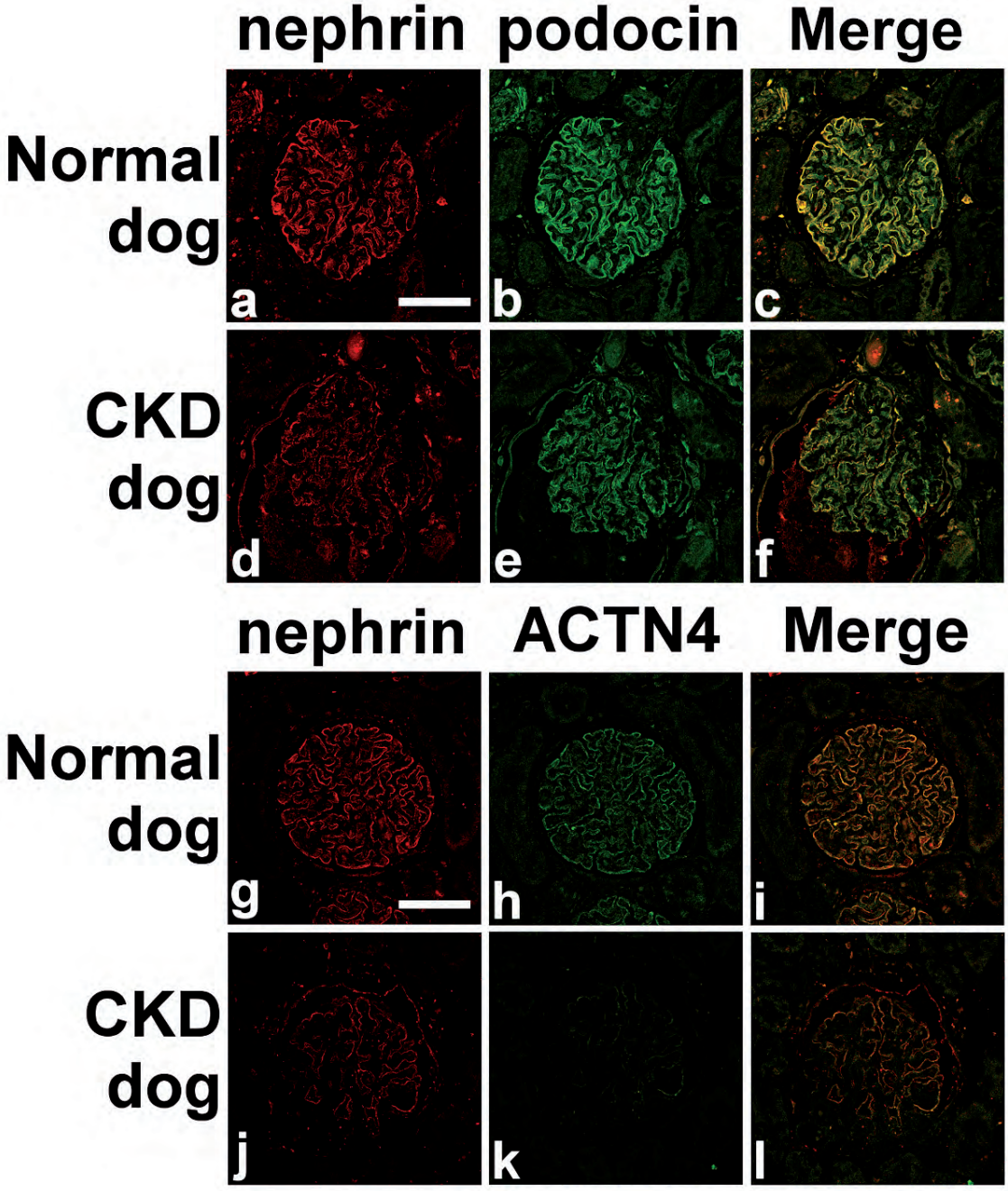

Fig. 4. Localization patterns of SD molecules in the kidneys of dogs. **a-l.** Show digital images of renal corpuscles in dog kidney sections stained with imunofluorescence dyes. In normal dogs, clear linear reactions of nephrin (red: TRITC), podocin (green: FITC), ACTN4 (green: FITC), and their merge image (orange) were detected parallel to the glomerular capillary **(a-c, g-i)**. The reaction patterns of these 3 molecules in CKD dogs changed from linear to irregular and granular, and their reaction intensities, especially of nephrin and ACTN4, were weaker in CKD animals than in normal animals **(d-f and j-l)**. Bars: 50 μm.

mRNA expression of WT1 and SD molecules in cats.

Table 4 summarizes the results of correlation analysis between the indices of podocyte number and protein and mRNA expression of SD molecules. In dogs, the indices of podocyte number were positively correlated with histoplanimetric scores and mRNA expression of nephrin (r=0.532, *P*=0.016; r=0.454, *P*=0.044, respectively). In cats, the indices of podocyte number were positively correlated with histoplanimetric scores of nephrin (r=0.654, *P*=0.040).

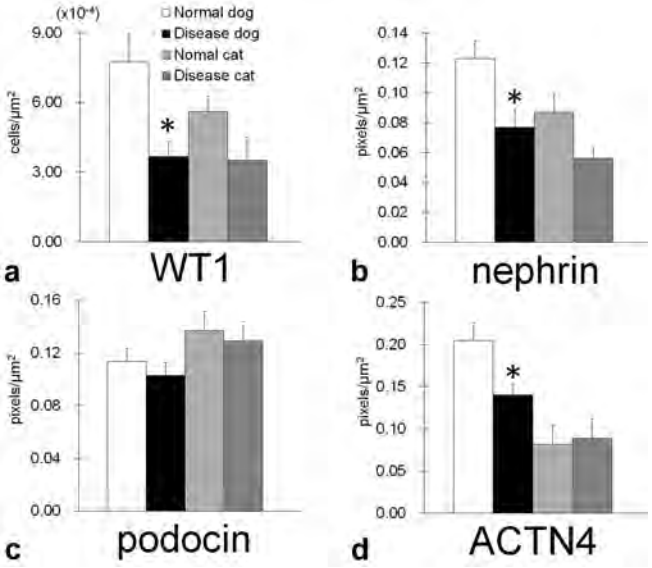

Fig. 5. Quantifications of WT1 and SD molecule protein expression in the kidneys of dogs and cats. Number of WT1-positive cells in the glomerulus **(a)**, and histoplanimetric scores of nephrin, podocin, and ACTN4 protein expression **(b, c, and d)** in dogs and cats. Values = means (standard errors). *: significant differences between normal and CKD animals (Mann-Whitney *U* test, *P*<0.05). n=13 (normal dogs), n=9 (CKD dogs), n=5 (normal cats), n=5 (CKD cats).

Urinary mRNA detections targeting podocyte markers

Fig. 7 shows the results of urinary mRNA detections targeting podocyte markers in CKD animals. In dogs, *WT1* (4/10), *NPHS2* (1/10), and *ACTN4* (7/10) were detected. In cats, *WT1* (4/10) and *ACTN4* (5/10) were detected. On the other hand, no *NPHS1*-specific band was detected in either dogs or cats.

Discussion

Podocytopenia in CKD of dogs and cats

Podocytopenia is a common feature of glomerular injury, and its association with renal dysfunctions, such as increase of proteinuria, has been reported in humans and in experimental rodents (Lemley et al., 2002; Suzuki et al., 2009). WT1 mainly localizes to the nucleus of podocytes. The number of WT1-positive cells is generally considered an index of podocyte numbers (Menini et al., 2007). Similar to these reports, WT1-positive cells in the glomerulus significantly decreased in CKD dogs. We confirmed pathological correlations between podocytopenia and canine CKD. In addition, WT1 acts as a transcription factor in the development and functional regulation of podocytes by regulating the expression of several genes, such as *podocalyxin and pax2* (Chugh, 2007). In addition, altered *WT1* mRNA expression also affects the development of several renal diseases. Briefly, *WT1* mutations are associated with the development of glomerulosclerosis, such as in Denys Drash and Frasier syndromes (Benetti et al., 2010). Moreover, reduction in *WT1* mRNA expression has been noted in glomerular diseases such as passive Heymann

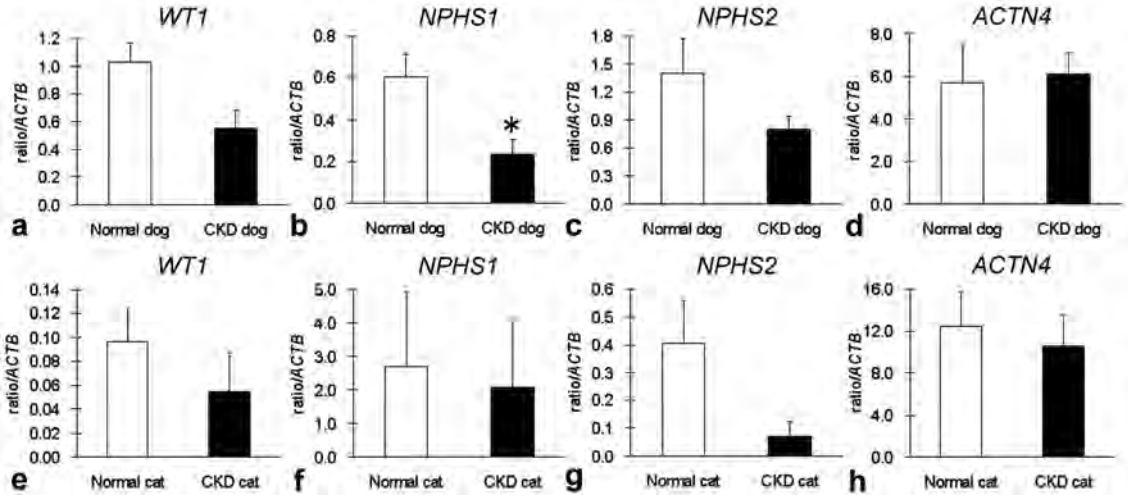

Fig. 6. Quantifications of WT1 and SD molecule mRNA expression in the kidneys of dogs and cats. Real-time PCR analysis of the mRNA expression of *WT1* (**a and e**), *NPHS1* (nephrin: **b and f**), *NPHS2* (podocin: **c and g**), and *ACTN4* (**d and h**) in dogs and cats. Raw values were normalized to those of *ACTB*. Values = means (standard errors). *: significant differences between normal and CKD animals (Mann-Whitney *U* test, *P*<0.05). n=13 (normal dogs), n=9 (CKD dogs), n=5 (normal cats), n=5 (CKD cats).

nephritis (Clement et al., 2007). Therefore, in dogs, a decreased number of WT1-positive cells might also reflect a decrease in WT1 expression, causing podocyte dysfunction and loss.

SD molecules in CKD of dogs and cats

Several studies have reported that a decrease in SD expression correlates with glomerular disease in humans and in experimental rodents (Kawachi et al., 2009). Morphometrical scores of nephrin and ACTN4, and *NPHS1* mRNA expression, in CKD dogs, were significantly lower than those in the normal group. However, no significant decrease was detected in cats. These results confirm the species-specific differences of pathogenesis in canine and feline CKD, and show that dog podocytes have high (and cat podocytes have low) sensitivities to cell injuries. Nephrin plays important roles not only in the components of SD but also in the regulation of podocyte cell signaling. Briefly, nephrin interacts with the p85 regulatory subunit of PI3K, recruits PI3K to the plasma membrane and stimulates PI3K-dependent AKT signaling, controlling cell growth, migration, and survival (Huber et al., 2003). ACTN4 has critical roles in maintaining the podocyte skeletal structure, colocalizes with actin bundles, and is required for ß1-integrin signaling and adhesion (Dandapani et al., 2007). Therefore, we hypothesize that nephrin and ACTN4 have roles in maintaining podocyte cell signaling and cytoskeletons, and decreases in their expression are critical for the development of podocyte injuries.

Interestingly, some studies suggest that epithelial-mesenchymal transition (EMT), which starts with a decrease in cell adhesion and changes in the cytoskeleton, is considered one of the trigger mechanisms of podocytopenia (Yamaguchi et al., 2009). In the analysis of podocyte EMT, a decrease in nephrin and ZO-1 and the induction of mesenchymal markers, such as desmin, fibronectin, matrix metalloproteinase-9, and alpha-smooth muscle actin, were observed (Li et al., 2008). Nephrin interacts with the actin polymerization complex via the adaptor protein Nck at the SD (Tryggvason et al., 2006), and ACTN4 bundles the actin cytoskeleton (Dandapani et al., 2007). Based on these findings, we believe that a decrease in SD molecules, including nephrin and ACTN4, might induce actin-related cytoskeletal changes of podocytes associated with early events of EMT, such as loss of adhesion to the GBM.

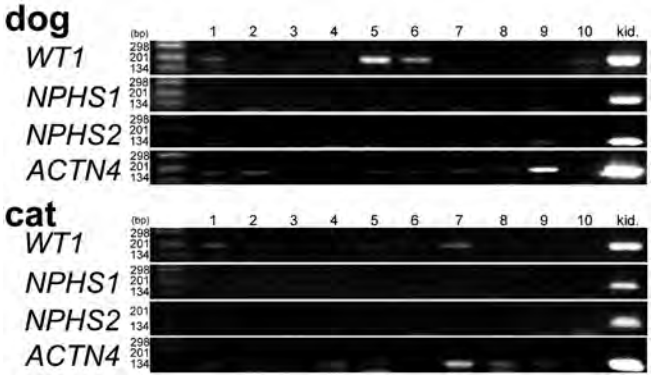

Fig. 7. Detections of urinary podocyte markers in CKD dogs and cats. PCR analysis of *WT1, NPHS1, NPHS2,* and *ACTN4 mRNA* from urine samples of CKD animals. Urinary sediments from 300 mL of urine from each animal were analyzed. Size markers are represented on the left. n=10 (CKD dogs and cats).

Pathological correlations between podocyte injuries and renal functions

Unexpectedly, no significant correlations between WT1 expression and renal dysfunctions were observed in either animal. On the other hand, Cre negatively and more strongly correlated with morphometrical scores of nephrin and ACTN4 and *NPHS1* mRNA expression in dogs than in cats. Furthermore, the indices of podocyte number correlated with nephrin expression (see Table 4). These results indicate that decreased expression of nephrin and ACTN4, rather than WT1 and podocin, is a sensitive indicator of developing podocyte injuries and glomerular dysfunctions in dogs. WT1 maintains podocyte homeostasis at the molecular upstream and also regulates the transcription of *NPHS1* expression (Wagner et al., 2004). Although podocytopenia is a final feature of podocyte injury, the dog samples used in this study were under various stages of CKD. Therefore, podocyte injuries, such as decreased expression of SD molecules and WT1, might correlate with other clinical parameters of early CKD stage. In the veterinary clinic, it is commonly believed that the most popular symptom of canine renal diseases is the appearance of proteinuria (Vaden et al., 2005). Furthermore, previous studies on cats clearly showed significant correlations between indices for renal dysfunctions, such as Cre level and TILs, characterized by an increase in alpha-smooth muscle actin–positive cells in the renal interstitium or renal fibrosis (Yabuki et al., 2010). These reports indicate that serological indices of renal dysfunctions, such as Cre level, correlate with TILs rather than glomerular lesions. TILs and a severe increase of clinical parameters such as Cre level could be detected in the late stages of CKD (Elliott and Barber, 1998; Nangaku, 2004). Therefore, early detection of podocyte injuries would lead to early diagnosis and prognosis for patients. To elucidate this point, it is necessary to evaluate the correlations between podocyte injuries and earlier clinical indices for renal dysfunctions, such as proteinuria or microalbuminuria.

Species-specific differences of CKD

Several studies have reported the differences in the pathological development of CKD between dogs and

cats. Briefly, approximately 52% of renal biopsy samples from diseased dogs had glomerular injuries (Macdougall et al., 1986). On the other hand, tubulointerstitial damage, including cell infiltrations, fibrosis, polycystic lesions, and necrosis, were commonly observed in feline renal disease (Elliott and Barber, 1998; Yabuki et al., 2010). In agreement with these reports, dogs showed more significant correlations between glomerular injuries and renal dysfunctions than those in cats. Although the reasons for the pathological species-specific differences in this study were unclear, TILs, such as infiltration of mononuclear cells, were commonly observed in CKD cat samples. These results might be indicative of the existence of cat-specific immune-mediated renal pathogenesis. In recent studies, significant correlations exist between CKD and feline immunodeficiency virus infection status, determined by positive test results for serum antibodies against feline immunodeficiency virus gp40 (White et al., 2010). In humans, immunodeficiency virus-associated nephropathy is caused by human immunodeficiency virus infections of renal tubules and podocytes (Shah et al., 2006). It is hypothesized that not only some factors derived from animals, but also environmental factors, including natural exposure to antigens, might affect species-specific differences of CKD pathogenesis.

Urinary podocytes

In humans, mRNA expression of podocyte markers such as *WT1*, *NPHS1*, *NPHS2*, and *ACTN4* were significantly increased in the urinary sediments of patients with diabetic nephropathy compared with healthy controls (Wang et al., 2008). In agreement with this report, mRNAs of podocyte markers, including *WT1*, *NPHS2* and *ACTN4*, with the exception of *NPHS1*, could be detected in urine of CKD animals. Interestingly, in these markers, *ACTN4* was detected at a high rate (dogs: 70%, cats: 50%). A previous study using a podocytopenic rat model suggested that urinary podocin and nephrin mRNA levels were significantly increased in the acute phase rather than in the chronic phase (Sato et al., 2009). Furthermore, the expression of nephrin mRNAs in urinary podocytes was decreased in the chronic phase compared with that in the acute phase (Sato et al., 2009). From these findings, although detection of urinary mRNA targeting podocyte markers has potential applications to the development of CKD diagnosis methods, it is essential to select several markers that can be adapted to both animal species and disease phases.

In conclusion, decreased numbers of WT1-positive podocytes and decreased expression of nephrin and ACTN4 were more closely associated with CKD in dogs than in cats. The importance of a species-specific CKD treatment is emphasized from these results, and evaluation of podocyte injuries with specific focus on these molecules has an important role in the development of treatments for early CKD.

Acknowledgments. This work was supported by grants from Grant-in-Aid for Young Scientists (Start-Up, no. 21880002), the Kuribayashi Foundation (no. 21-1) and research expense of public offering type project in Hokkaido University (2010s).

References

Benetti E., Caridi G., Malaventura C., Dagnino M., Leonardi E., Artifoni L., Ghiggeri G.M., Tosatto S.C. and Murer L. (2010). A novel WT1 gene mutation in a three-generation family with progressive isolated focal segmental glomerulosclerosis. Clin. J. Am. Soc. Nephrol. 5, 698-702.

Caridi G., Perfumo F. and Ghiggeri G.M. (2005). NPHS2 (Podocin) mutations in nephrotic syndrome. Clinical spectrum and fine mechanisms. NPHS2 (Podocin) mutations in nephrotic syndrome. Clinical spectrum and fine mechanisms. Pediatr. Res. 57, 54-61.

Chugh S.S. (2007). Transcriptional regulation of podocyte disease. Transl. Res. 149, 237-242.

Clement L.C., Liu G., Perez-Torres I., Kanwar Y.S., Avila-Casado C. and Chugh S.S. (2007). Early changes in gene expression that influence the course of primary glomerular disease. Kidney Int. 72, 337-347.

Dandapani S.V., Sugimoto H., Matthews B.D., Kolb R.J., Sinha S., Gerszten R.E., Zhou J., Ingber D.E., Kalluri R. and Pollak M.R. (2007). Alpha-actinin-4 is required for normal podocyte adhesion. J. Biol. Chem. 282, 467-477.

Elliott J. and Barber P.J. (1998). Feline chronic renal failure: clinical findings in 80 cases diagnosed between 1992 and 1995. J. Small Anim. Pract. 39, 78-85.

Hara M., Yanagihara T., Hirayama Y., Ogasawara S., Kurosawa H., Sekine S. and Kihara I. (2010). Podocyte membrane vesicles in urine originate from tip vesiculation of podocyte microvilli. Hum. Pathol. 41, 1265-1275.

Huber T.B., Hartleben B., Kim J., Schmidts M., Schermer B., Keil A., Egger L., Lecha R.L., Borner C., Pavenstädt H., Shaw A.S., Walz G. and Benzing T. (2003). Nephrin and CD2AP associate with phosphoinositide 3-OH kinase and stimulate AKT-dependent signaling. Mol. Cell. Biol. 23, 4917-4928.

Juhila J., Lassila M., Roozendaal R., Lehtonen E., Messing M., Langer B., Kerjaschki D., Verbeek J.S. and Holthofer H. (2010). Inducible nephrin transgene expression in podocytes rescues nephrin-deficient mice from perinatal death. Am. J. Pathol. 176, 51-63.

Kaplan J.M., Kim S.H., North K.N., Rennke H., Correia L.A., Tong H.Q., Mathis B.J., Rodríguez-Pérez J.C., Allen P.G., Beggs A.H. and Pollak M.R. (2000). Mutations in ACTN4, encoding alpha-actinin-4, cause familial focal segmental glomerulosclerosis. Nat. Genet. 24, 251-256.

Kawachi H., Suzuki K., Miyauchi N., Hashimoto T., Otaki Y. and Shimizu F. (2009). Slit diaphragm dysfunction in proteinuric states: identification of novel therapeutic targets for nephrotic syndrome. Clin. Exp. Nephrol. 13, 275-280.

Krawiec D.R. and Gelberg H.B. (1989). Chronic renal disease in cats. In: Current veterinary therapy X: Small animal practice. Kirk R.W. (ed). WB Saunders Co. Philadelphia. pp 1170–1173.

Lemley K.V., Lafayette R.A., Safai M., Derby G., Blouch K., Squarer A.

and Myers B.D. (2002). Podocytopenia and disease severity in IgA nephropathy. Podocytopenia and disease severity in IgA nephropathy. Kidney Int. 6, 1475-1485.

Li Y., Kang Y.S., Dai C., Kiss L.P., Wen X. and Liu Y. (2008). Epithelial-to-mesenchymal transition is a potential pathway leading to podocyte dysfunction and proteinuria. Am. J. Pathol. 172, 299-308.

Luimula P., Ahola H., Wang S.X., Solin M.L., Aaltonen P., Tikkanen I., Kerjaschki D. and Holthöfer H. (2000). Nephrin in experimental glomerular disease. Kidney Int. 58, 1461-1468.

Lund E.M., Armstrong P.J., Kirk C.A., Kolar L.M. and Klausner J.S. (1999). Health status and population characteristics of dogs and cats examined at private veterinary practices in the United States. J. Am. Vet. Med. Assoc. 214, 1336–1341.

Lysaght M.J. (2002). Maintenance dialysis population dynamics: current trends and long-term implications. J. Am. Soc. Nephrol. 13, 37-40.

Macdougall D.F., Cook T., Steward A.P. and Cattell V. (1986). Canine chronic renal disease: prevalence and types of glomerulonephritis in the dog. Kidney Int. 29, 1144-1151.

Menini S., Iacobini C., Oddi G., Ricci C., Simonelli P., Fallucca S., Grattarola M., Pugliese F., Pesce C. and Pugliese G. (2007). Increased glomerular cell (podocyte) apoptosis in rats with streptozotocin-induced diabetes mellitus: role in the development of diabetic glomerular disease. Diabetologia 50, 2591-2599.

Nangaku M. (2004). Mechanisms of tubulointerstitial injury in the kidney: final common pathways to end-stage renal failure. Intern. Med. 43, 9-17.

Patrakka J., Kestilä M., Wartiovaara J., Ruotsalainen V., Tissari P., Lenkkeri U., Männikkö M., Visapää I., Holmberg C., Rapola J., Tryggvason K. and Jalanko H. (2000). Congenital nephrotic syndrome (NPHS1): features resulting from different mutations in Finnish patients. Kidney Int. 58, 972-980.

Roselli S., Heidet L., Sich M., Henger A., Kretzler M., Gubler M.C. and Antignac C. (2004). Early glomerular filtration defect and severe renal disease in podocin-deficient mice. Mol. Cell. Biol. 24, 550-560.

Sato Y., Wharram B.L., Lee S.K., Wickman L., Goyal M., Venkatareddy M., Chang J.W., Wiggins J.E., Lienczewski C., Kretzler M. and Wiggins R.C. (2009). Urine podocyte mRNAs mark progression of renal disease. J. Am. Soc. Nephrol. 20, 1041-1052.

Shah S.N., He C.J. and Klotman P. (2006). Update on HIV-associated nephropathy. Curr. Opin. Nephrol. Hypertens. 15, 450-455.

Suzuki T., Matsusaka T., Nakayama M., Asano T., Watanabe T., Ichikawa I. and Nagata M. (2009). Genetic podocyte lineage reveals progressive podocytopenia with parietal cell hyperplasia in a murine model of cellular/collapsing focal segmental glomerulosclerosis. Am. J. Pathol. 174, 1675-1682.

Tryggvason K., Pikkarainen T. and Patrakka J. (2006). Nck links nephrin to actin in kidney podocytes. Cell 125, 221-224.

Vaden S.L., Levine J.F., Lees G.E., Groman R.P., Grauer G.F. and Forrester S.D. (2005). Renal biopsy: a retrospective study of methods and complications in 283 dogs and 65 cats. J. Vet. Intern. Med. 19, 794-801.

Wagner N., Wagner K.D., Xing Y., Scholz H. and Schedl A. (2004). The major podocyte protein nephrin is transcriptionally activated by the Wilms' tumor suppressor WT1. J. Am. Soc. Nephrol. 15, 3044-3051.

Wang G., Lai F.M., Lai K.B., Chow K.M., Kwan B.C., Li P.K. and Szeto C.C. (2008). Urinary messenger RNA expression of podocyte-associated molecules in patients with diabetic nephropathy treated by angiotensin-converting enzyme inhibitor and angiotensin receptor blocker. Eur. J. Endocrinol. 158, 317-322.

White K.E. and Bilous R.W. (2004). Estimation of podocyte number: a comparison of methods. Kidney Int. 66, 663-667.

White J.D., Malik R., Norris J.M. and Malikides N. (2010). Association between naturally occurring chronic kidney disease and feline immunodeficiency virus infection status in cats. J. Am. Vet. Med. Assoc. 236, 424-429.

Yabuki A., Mitani S., Fujiki M., Misumi K., Endo Y., Miyoshi N. and Yamato O. (2010). Comparative study of chronic kidney disease in dogs and cats: induction of myofibroblasts. Res. Vet. Sci. 88, 294-299.

Yamaguchi Y., Iwano M., Suzuki D., Nakatani K., Kimura K., Harada K., Kubo A., Akai Y., Toyoda M., Kanauchi M., Neilson E.G. and Saito Y. (2009). Epithelial-mesenchymal transition as a potential explanation for podocyte depletion in diabetic nephropathy. Am. J. Kidney Dis. 54, 653-664.

Accepted March 28, 2011